Published in final edited form as:
Cancer Biomark. 2008 ; 4(4-5): 251–262.

The Role of Magnetic Resonance Imaging (MRI) in Prostate Cancer Imaging and Staging at 1.5 and 3 Tesla : The Beth Israel Deaconess Medical Center (BIDMC) Approach

B. Nicolas Bloch, MD[*], **Robert. E. Lenkinski, PhD**, and **Neil M. Rofsky, MD**
Department of Radiology, MRI, Beth Israel Deaconess Medical Center and Harvard Medical School, Boston, MA 02215, USA

Abstract

Management decisions for patients with prostate cancer present a dilemma for both patients and their clinicians because prostate cancers demonstrate a wide range in biologic activity, with the majority of cases not leading to a prostate cancer related death. Furthermore, the current treatment options have significant side effects, such as incontinence, rectal injury and impotence. Key elements for guiding appropriate treatment include: distinction of organ-confined disease from extracapsular extension (ECE); and determination of tumor volume and tumor grade, none of which have been satisfactorily accomplished in today's pre-treatment paradigm. Magnetic resonance imaging (MRI) has the capability to assess prostate tissue, both functionally and morphologically. MRI as a staging tool has not shown enough consistency or sufficient accuracy for widespread adoption in clinical practice; yet, recent technical developments in MRI have yielded improved results. At our institution we have combined the use of new endorectal 3 Tesla MRI technology, T2-weighted, and high spatial resolution dynamic-contrast enhanced (DCE) MRI to non-invasively assess the prostate with higher signal-to-noise ratio and spatial resolution than previously achieved. This approach allows assessment of prostate-tissue morphology and kinetics, thus providing a non-invasive tool for tumor detection and staging and, consequently, directing biopsy and treatment specifically to diseased areas for a pre-treatment evaluation that can assist in the rational selection of patients for appropriate prostate cancer therapy.

Keywords

Prostate Cancer; Staging; Prostate Cancer Imaging; MR Imaging (MRI); Dynamic Contrast Enhanced MRI; Extracapsular Extension; Local Recurrence; Repeat Negative Biopsy; Anterior Tumors

Introduction

The American Cancer Society estimates that there will be about 218,890 new cases of prostate cancer in the United States in the year 2007[1]. Approximately 30,870 men will die of this disease. Prostate cancer is the second leading cause of cancer death in men, exceeded only by lung cancer. While one man in six will get prostate cancer during his lifetime, only one man in 32 will die of this disease [2]. Due to increased prostate cancer screening using serum prostate-specific antigen (PSA) and transrectal ultrasound (TRUS) guided biopsy, prostate cancer patients are being identified at an earlier and potentially treatable stage [3]. The

*Corresponding author: B. Nicolas Bloch, M.D., Department of Radiology, Beth Israel Deaconess Medical Center, 330 Brookline Ave. E/Dana-705b, Boston, Mass. 02215, U.S.A., nbloch@bidmc.harvard.edu.

importance and impact of prostate cancer will increase rapidly in the next decade. As the *baby-boomer* generation ages, it is expected that the incidence of prostate cancer will more than double in the US, with a projected number of 450,000 men to be diagnosed in 2015.

Management decisions for patients with prostate cancer are complicated and present a dilemma for both patients and their clinicians as prostate cancers demonstrate a wide range of biologic activity with the majority of cases not leading to a prostate cancer-specific death. Furthermore, the current treatment options for men with localized prostate cancer are aggressive and have significant side effects, such as incontinence, rectal injury and impotence. Thus it is clear that the challenges to the medical research community are to accurately predict a given prostate cancer's behavior to, select those patients who require therapy and to treat the cancer with the appropriate level of intensity while preserving the patient's quality of life.

Prostate Cancer Diagnosis, Prognosis and Treatment

Prostate cancer is one of the few cancers that can grow so slowly that they never threaten the lives of some patients. Yet, if the cancer does metastasize, the disease becomes lethal, as there is currently no cure. At present, predictions of the course of the disease in an individual patient using current prognostic markers have substantial limitations [4–7]. Thus, while a broad spectrum of approaches, from "watchful waiting" and hormone deprivation therapy to surgical, radiation, and cryosurgical therapies, are available, it is not a simple task to assign an individual patient to the most appropriate treatment strategy. Clinical (digital rectal exam (DRE)), pathologic (histologic grade from biopsy, and number and percentage of positive biopsies) [8], and biochemical parameters in serum (PSA, PAP) [9–12] or in tissue (MIB-1, bcl-2, p53, CD34) [13–17] can aid in assessing the extent and aggressiveness of the disease. However, these are often inaccurate or inadequate, particularly when used alone in individual patients for both pre- and post-treatment assessments [4,5] [18].

Additionally, with early detection there has also been increased interest in focal "disease-targeted" therapies, including interstitial brachytherapy, intensity-modulated radiotherapy, focal cryosurgery, and radiofrequency ablation which can potentially reduce treatment-related morbidity and allow patients to maintain their quality of life [19–24]. These therapies require an improved knowledge of the location and spatial extent of the disease within the gland. Finally, the long natural history of prostate cancer and the increasingly younger age of patients at the time of detection underscore the need for individually adjusted treatment decisions and regimes [25,26].

Improved screening of prostate cancer over the past decade has been achieved using prostate specific antigen (PSA) and digital rectal examinations (DRE). However, only a fraction of the men diagnosed each year with prostate cancer will demonstrate clinical progression during their lifetimes. Positive screening prompts a subsequent workup that emphasizes the detection and staging of the carcinoma. Traditional evaluations using the Gleason score from biopsy samples in conjunction with PSA assessments and DRE results, both individually and collectively, have limitations. The commonly used Partin tables, derived from these evaluations, primarily serve as a counseling tool regarding the probability of an individual tumor being at a specific pathologic stage rather than as decisive information for the individual. Key elements for guiding appropriate treatments in the individual include: distinction of organ-confined disease from extracapsular extension (ECE), a determination of total tumor burden, and a determination of tumor grade, none of which have been satisfactorily accomplished in today's pre-treatment paradigm [27]. Thus, a more comprehensive and objective means to characterize prostate cancer after its detection and prior to therapy would be very useful for clinical practice. Recent advances in MRI/MRS of the prostate are beginning to meet these challenges.

Imaging of the Prostate

Transrectal Ultrasound (TRUS)

Prostate cancer appears as a hypoechoic lesion in the peripheral zone on transrectal ultrasound (TRUS). However, many cancers are undetectable and are presumably isoechoic. In the American Cancer Society prostate screening study of 2427 men, a total of 52 cancers were detected [28]. Of these, TRUS detected 44 (85%), indicating its limited sensitivity. In addition, TRUS is not specific. In this same study, 396 of 2425 men had a suspicious ultrasound, but only 44 of these men had prostate cancer. Power Doppler techniques applied to TRUS have failed to provide substantial improvements [29,30], and recently published data suggests better results with DCE-MRI in a direct comparison study [31].

Computed Tomography (CT)

CT lacks sufficient soft tissue contrast for detection of cancer or local staging and has its greatest value in the evaluation of distant spread of disease [32].

MRI of the Prostate

Inherent to magnetic resonance (MR) technology is the capability to assess prostate cancer functionally and morphologically. While an emphasis on MR as a staging tool has not yielded consistent or sufficient accuracy for widespread adoption in clinical practice, recent developments in MR technology have yielded improved capabilities and new possibilities. The development of specific hardware, such as high-field scanners (3 Tesla), endorectal coils and dedicated phased array coils for the torso, as well as advances in pulse sequences (e.g., spoiled gradient echo and fast spin echo methods) have increased the potential for utilizing MRI in clinical assessment of prostate disease. The large array of techniques, including T1-weighted images, T2-weighted images, dynamic contrast enhanced (DCE) T1-weighted images, MR spectroscopy, diffusion weighted images and others, provides many opportunities to evaluate biologic processes. For prostate cancer, T2-weighted images are currently the most commonly used technique [33,34].

T2-weighted (T2W) MRI

The use of T2W MRI has largely focused on staging, since the low signal features used to identify cancer are not specific [32]. The literature reports on the staging accuracy of MRI are variable. Some studies have reported values as high as 88%, with most studies ranging between 57–82 %[34]. Seltzer et al [35] showed that the most important single factor in determining reader accuracy was the experience of the reader (inexperienced readers had an accuracy of 67%, experienced readers 87%). From a technical point of view, this result is encouraging because it shows that once the MRI protocol has been established and sites are capable of producing reasonable quality MRI studies, the interpretation of the images becomes the limiting factor. However, it is recognized that MRI, in its current form, may have insufficient tissue contrast or resolution to detect microscopic foci of adenocarcinoma. This may result in limited correlations to histopathology. But, such a limitation may not be critical for patient management, since it has been shown that there is no adverse effect on five-year post-operative disease recurrence in patients with focal capsular penetration [36]. Nevertheless, the value of T2-W MRI of the prostate depends on the visualization of the tumor and prostate capsule and the ability to assess the spatial relationships to each other. This in turn is greatly influenced by the achievable spatial resolution and tissue contrast, leading some investigators to conclude that higher spatial resolution facilitates better clinical performance of MRI of the prostate. Currently, the best spatial resolution at 1.5T with reasonable SNR is achieved with a FOV of 12–14 and a slice thickness of 3 mm and a matrix of 256 ×192–256 resulting in voxel sizes of 0.66–1.12 mm3. The excellent spatial resolution achieved with endorectal coil 3T MRI with

at least halving the voxel size (voxel size, 0.35 mm3 *v* 0.66–1.12 mm3), reveals pathoanatomic details on T2-W images not seen at 1.5T or 3T without endorectal coil.[37]

Magnetic resonance spectroscopic imaging (MRS)

MRS is emerging as a useful technique for local evaluation of prostate cancer extent and aggressiveness. MRS facilitates the differentiation of normal and altered tissue metabolism, and is therefore different to other imaging methods that only assess abnormalities of structure or perfusion. The primary MRS technique that is currently available commercially utilizes the point-resolved spectroscopy (PRESS) sequence, with spectral spatial pulses and very selective outer voxel suppression for water and lipid suppression.[38–42] The authors of a recently published study came to the conclusion that the addition of MR spectroscopic imaging to MR imaging significantly improves characterization of peripheral zone prostate tissue as benign or malignant; improved performance is obtained when both data sets are interpreted in an integrated fashion. [43]

Diffusion Weighted MRI of the Prostate

Diffusion-weighted and quantitative diffusion MR imaging (DWI) using apparent diffusion coefficient (ADC) mapping generates tissue contrast reflecting water molecular diffusion. Diffusion MR is commonly used for assessing acute stroke in the brain [44,45]. More recently, it has been suggested that diffusion imaging may also play a role in the early detection of tumor response to therapy [46–48].

Standard diffusion studies in humans have primarily employed single-shot echo planar imaging (EPI), which is vulnerable to chemical shift and susceptibility artifacts, issues which are quite relevant to body imaging. The line scan diffusion (LSD) imaging technique can reduce these artifacts [49–51]. Preliminary results with LSD have suggested a reduction of ADC values in prostate tumor vs. normal tissue in the peripheral zone [52]. However, LSD has relatively long acquisition times making it difficult to achieve reasonable spatial resolution in a feasible time period. The introduction of 3 Tesla magnets, opens new possibilities for DWI, as the higher field strength allows faster acquisitions, but this must tempered against the additional challenges imparted by EPI related artifacts at 3T.

Dynamic contrast-enhanced (DCE) MRI

Both microvessel density (MVD) and the expression of angiogenic factors have been evaluated as prognostic factors in patients with prostate cancer. MVD has been correlated with clinical and pathological stage, metastasis and histological grade in prostate cancer [53–58]. MVD has also been correlated with disease-specific survival and progression after treatment [53,54], although some controversy exists [59–62]. Moreover, recent data suggest that DCE MRI can provide important information about individual MVD in prostate cancer [63]. Thus, there are biological features associated with prostate cancer that can be demonstrated with DCE MRI for further disease characterization.

Kinetic Analyses of DCE MRI

Quantitative evaluations following intravenous administration of contrast media use pharmacokinetic modeling techniques that are usually applied to concentration changes in tissue contrast agents. Signal intensity changes observed during dynamic acquisition are used to estimate contrast agent concentration *in vivo* [64,65]. Concentration-time curves are then mathematically fitted using one of a number of recognized pharmacokinetic models to derive quantitative kinetic parameters [66]. Examples of modeling parameters include the volume transfer constant of the contrast agent (K^{trans} - formally called permeability-surface area product per unit volume of tissue), leakage space as a percentage of unit volume of tissue

(v_e) and the rate constant (k_{ep} also called K_{21}). These standard parameters are related mathematically ($k_{ep} = K^{trans} / v_e$) [67].

Accepting that there are outstanding issues with regard to model-based assumptions and the measurement of tissue contrast agent concentration, quantitative kinetic parameters, such as K^{trans} and v_e, do allow comparisons to be made between and within patients and different imaging centers and provide insights into underlying tissue physiological processes.

Temporal and Spatial Resolution in DCE MRI

To date, contrast enhanced MRI has been performed in either a static mode in which T1-weighted images are acquired 1–2 minutes after contrast administration over a long period of time (3–4 minute acquisition) or in a rapid, dynamic mode capturing multiple time points during and after contrast media administration. DCE MR imaging offers multiple samples of anatomy and pathology throughout contrast administration and provides an opportunity to assess contrast kinetics. During recent years contrast kinetic evaluations have become an important focus for the assessment of cancer and new cancer therapies, as summarized by Brasch, et al. [68]. Imaging constraints present challenges to achieving high spatial and temporal resolution information, simultaneously. High spatial resolution allows for more complete sampling of the structures of interest and better detail of the anatomy and pathology. High temporal resolution provides a more frequent update of the contrast dynamics and can facilitate quantitative kinetic analyses [69].

Recognizing that tumor heterogeneity can not be appreciated with low spatial, high temporal resolution and responding to the limited sampling of data possible with such an approach, Degani and associates have focused on achieving an acceptable trade-off between temporal and spatial resolution for breast cancer [70]. Endorectal coil 3T MRI enables dynamic contrast enhanced studies at a much higher spatial resolution as compared with 1.5T, achievable without compromises in temporal resolution. This paves the way for dynamic studies with high patho-anatomic detail at an optimal temporal resolution for kinetic analysis.[37]

DCE MRI and Detection of ECE of Prostate Cancer

In previous reports investigators have suggested that gadolinium-enhanced or dynamic endorectal MRI may be useful for the evaluation of extracapsular extension of prostate cancer in selected patients [71–73]. On the other hand, Quinn *et al*. reported that gadolinium enhancement was of no benefit in the staging of prostate cancer [74]. All of these techniques employed 2D acquisition techniques with relatively thick (>5mm) sections and intersection gaps resulting in a substantial degree of image undersampling of the gland. Prior dynamic contrast enhanced imaging has focused on low spatial resolution and high temporal resolution [75,76]. However, tumor detection rates were still limited: the overall sensitivity, specificity, and accuracy of the detection of cancer in the prostate gland was 59%, 88%, and 72%, respectively [76].

One reason that the promise of DCE MRI to improve the determination of ECE in prostate has not been realized may result from the limited spatial resolution used with prior studies. Such an approach is likely insufficient to assist with the fine morphologic details required for detection of ECE.

MRI of the Prostate at Beth Israel Deaconess Medical Center – Boston

At our institution we have combined the use of 3T clinical magnetic resonance (MR) technology, T2-weighted and high spatial resolution DCE MRI, and an endorectal-coil (ERC) probe in order to non-invasively obtain images of the prostate gland with higher signal-to-noise resolution and better spectral dispersion than has been previously achieved at 1.5T. The

incremental value of high spatial resolution DCE MRI was shown recently [77]. This imaging strategy acquires higher-resolution images with smaller voxel sizes than has been possible with prior MR technology and more comprehensive tissue sampling compared to other pre-surgical assessments. This methodology makes it feasible to assess prostate-tissue morphology and additional features of prostate cancer such as tissue kinetics, and the vascular microenvironment, providing a non-invasive tool to: 1) detect extra-capsular spread; 2) detect specific areas within the prostate that harbor cancer; and 3) direct biopsy and treatment specifically to diseased areas, resulting in a pre-treatment evaluation that can assist in the rational selection of patients to undergo appropriate and definitive therapy for prostate cancer. While diffusion weighted MRI (DWI) has been added to our T2-W and high spatial resolution DCE MRI protocol, we are still validating its contribution.

Currently at our institution, patients are referred for MR of the prostate for two main reasons: pretherapeutical staging, or local recurrence after definite treatment. Recently, we have seen a growing number of referrals to define a biopsy target for patients with rising PSA and repeat negative biopsies, as well as to designate a dominant nodule location prior to Brachytherapy, and external beam radiation therapy (EBRT). Preliminary data suggests that contrast enhanced MRI has value for brachytherapy post-treatment evaluation and planning. [78]

MR Protocols

All patients, whether they are evaluated for pre- or posttherapeutic assessment, undergo the same standardized comprehensive MR protocol at BIDMC:

Patient Preparation

Patients are asked to refrain from ejaculation for three (3) days preceding the exam to ensure optimal distension of the seminal vesicles. A sodium phosphate enema is administered on the day of the study in order to minimize fecal residue in the rectum. A1mg glucagon i.m. injection is administered to reduce peristaltic motion. The ERC (MRInnervu, Medrad, Pittsburgh, PA) is inserted into the rectum and connected to a pelvic phased-array coil with a coupling device to combine the surface phased array coil with the endorectal coil. Barium suspension is used to fill the ERC balloon, with a typical volume of 80cc's, however, adjusted for patient tolerance. The use of Barium reduces susceptibility effects when compared to the use of air and should improve MRS and DWI results.[79]

MR imaging is performed on a 3.0-T MR imaging system (Genesis Signa LX Excite, General Electric, Milwaukee, WI), and combined images are obtained. The coil position is verified with sagittal T2-weighted localizer images and adjusted, if needed, so that the prostate gland is optimally situated with respect to the coil.

The imaging parameters are summarized in Table 1.

T2W images—transverse and coronal fast spin-echo T2-weighted images are obtained from below the prostatic apex to above the seminal vesicles using the following parameters: repetition time msec/echo time msec (effective) 4,500–7600/165, 2.0–2.2mm section thickness and no intersection gap, 3 averages, 14-cm field of view, 256 × 192 matrix, and no phase wrap. A unique attribute of this protocol is the use of thinner sections than have been the previous routine. This results in 30% – 50% more sampling of the gland compared to the traditional 3–4 mm section approach. The phase encoding direction is left-right.

Three-dimensional (3D) T1-weighted (T1W) gradient echo (GRE) images—These are acquired prior to, during, and after contrast injection. DCE images are obtained after bolus injection of gadopentetate dimeglumine (Magnevist®; Berlex Laboratories, Wayne, NJ) at a

dose of 0.1 mmol / kg of body weight administered with a mechanical injection system (Spectris® MR Injection System, MEDRAD, Pittsburgh, PA) at a flow rate of 4ml/sec. The imaging parameters of the 3D GRE sequence are: TR/TE 9.3/4.2 msec, flip angle 18°, FOV 14cm, matrix 256 × 224, ST: 2.0–2.6mm, no phase wrap, which can be obtained with a temporal resolution of approximately 1 minute, 35 seconds. Two pre-contrast and five post-contrast sequential acquisitions are obtained.

For the pre-contrast scans, the first is used to ensure relevant anatomic coverage; the second is used as part of a continuous series of pre- and post-acquisitions in which the instrument settings (gain and attenuation values) are identical. Contrast injection is initiated during the last 10 seconds of the 2nd pre-contrast acquisition.

Echo-planar Diffusion weighted images (EPI)—transverse DWI with whole gland coverage is performed with the following parameters: TR/TE = 6500/80.6 msec; parallel imaging factor = 2; averages= 2 NEX; FOV 24cm; slice thickness = 3 thick; matrix = 256 × 192; scan time: 7:12 min; B-value= 0,1000; number of directions = 25. Instead of using more averages (NEX) to gain adequate signal at this high spatial resolution, we choose 25 directions, to achieve not only a better signal-to-noise ratio, but also improved results in diffusion tensor imaging and anisotropic maps as well as enhanced contrast in the ADC maps.

Axial spin-echo or fast spin-echo T1W images—T1-weighted images from the aortic bifurcation to the symphysis pubis. TR/TE = 600–700/−12 msec. Slice thickness 4–6 mm. Interslice gap 0–1 mm. Matrix 256 × 192. Frequency direction transverse (to prevent obscuration of pelvic nodes by endorectal coil motion artifact). Number of excitations = 1. FOV 20–32 cm.

MR Applications at the BIDMC

MR staging and detection of Extracapsular Disease at BIDMC—A study that combined a T2-W and DCE-MR protocol revealed a mean sensitivity, specificity, positive predictive value (PPV) and negative predictive value (NPV) for the detection of ECE of 86%, 95%, 90% and 93%, respectively [77],. The sensitivity for ECE MRI was improved by more than 25% using the combined T2-W/DCE-MRI approach compared to T2-W MRI alone. The combined T2-W/DCE-MRI approach had a mean overall staging accuracy of 95%, as determined by the area under the receiver operating characteristic curve. Staging results were significantly improved ($p < .05$) using the combined approach compared to T2-W MRI alone. Figure 1 shows an example of MRI at 3T performed for pretherapeutic evaluation and staging.

MR imaging for Local Recurrence of Prostate Cancer at the BIDMC—Without a direct, objective means to evaluate local recurrence, nomograms have been developed to assist in treatment decisions[80–82].

These nomograms are based on clinical parameters, such as clinical stage and grade before prostatectomy/radiation therapy, PSA doubling time, and time between therapy and PSA relapse, nomograms estimate the *probability* of local and distant recurrence based on averages over large numbers of patients. Thus, these parameters are of limited benefit to the individual seeking advice on the approach to *his* disease. Hence, both patient and clinician are forced to make important choices among local and systemic therapies without knowing the true localization and the extent of the recurrent disease. Essential questions to be answered are: 1) is the PSA relapse caused by local or distant recurrence? 2) Is the tumor multi-focal, and if so, how many tumors are there within the prostate (bed)? 3) What is the total volume of the recurrent cancer? 4) Have malignant cells already spread to the nearby lymph nodes? Without

answers to these questions, patients and physicians are relegated to critical decisions based on statistical probabilities.

Prostate cancer has many expressions and needs to be addressed on an individual basis for optimized management in each patient. Conventional MR imaging shows limited results in local recurrence detection, influenced by the negative impact of post-interventional changes on tumor detection. T2-W MRI cannot not readily distinguish between the low signal intensities of fibrotic changes, scar tissue and cancerous tissue after prostatectomy, or the low signal intensities of post radiation changes. DCE-MRI, however, is able to differentiate between cancer tissue and fibrotic or radiated tissue based on the enhancement features. Figure 2 shows an example of high resolution DCE-MRI and detection of local recurrence after Brachytherapy at 3T.

The patient underwent Brachytherapy seed implantation 3 years prior to the MRI, and was referred after PSA-relapse. Note the local recurrence in a “cold spot” where there is a relative lack of seeds, in the posterior right peripheral zone. Note the seeds visualized as small signal voids (black) in post-contrast image (Figure 2b) and the clear visualization of the cancer on the parametric map (Figure 2c). The MRI diagnosis was confirmed by targeted biopsy.

Prostate Cancer Detection and Localization in Patients with Repeat Negative Biopsies—In an ongoing prospective study we are currently investigating the value of high spatial resolution dynamic contrast enhanced (DCE-) with high spatial resolution T2-weighted (T2-W) endorectal (ER) coil magnetic resonance imaging (MRI) at 3 Tesla for detection and localization of prostate cancer in patients with repeat negative biopsies and rising prostate specific antigen (PSA), using histopathology of the subsequent biopsy as the reference standard. The preliminary results are promising. MR based biopsy detected prostate cancer in >50% of patients, with the tumor being located in the anterior gland, as predicted by MRI, in the majority of the cases. These results suggest an improvement over previously reported results of randomly performed repeat biopsies or targeted sextant biopsies with emphasis on anterior and lateral tissue sampling [83–85]. This preliminary data suggests that MRI can assist in the reduction of repeat negative biopsies in patients with rising PSA. Figure 3 shows a patient with 3x repeat negative biopsies (total 63 negative cores) and a rising PSA (27 ng/ml) prior to the MR exam. A targeted ultra-sound guided biopsy based on the MRI findings confirmed cancer in the anterior gland. Consequently, the patient underwent prostatectomy.

Summary

At Beth Israel Deaconess Medical Center a 3T high spatial resolution T2-W and DCE-MRI protocol is assisting clinicians in their efforts to more objectively and rationally select appropriate treatment for the individual patient with prostate cancer based on an improved capacity for tumor detection and staging. MRI is increasingly relied upon at our institution to detect cancer and target in patients with repeat negative biopsies and rising PSA levels. As we gain more experience with this protocol, we anticipate undertaking systematic studies which involve correlating the MRI features (MRI phenotype) with underlying gene expression and protein expression profiles (genotype). Our preliminary results in this area have shown a great deal of promise in establishing which features can become true, validated, biomarkers for cancer and its individual biological behavior.[86]

Acknowledgement

B.N.B., R.E.L. and N.M.R. supported, in part, by grant 5R01CA116465-02 from the National Institutes of Health. B.N.B. is supported, in part, by Bayer Healthcare Pharmaceuticals.

References

1. Leading Sites of New Cancer Cases and Deaths—2007. Estimates. Cancer Facts & Figures, American Cancer Society. 2007
2. Website ACS. Overview: Prostate Cancer. American Cancer Society. 2004
3. Han M, Partin AW, Piantadosi S, Epstein JI, Walsh PC. Era specific biochemical recurrence-free survival following radical prostatectomy for clinically localized prostate cancer. J Urol 2001;166(2): 416–419. [PubMed: 11458039]
4. Steuber T, Karakiewicz PI, Augustin H, Erbersdobler A, Lange I, Haese A, Chun KH, Walz J, Graefen M, Huland H. Transition zone cancers undermine the predictive accuracy of Partin table stage predictions. J Urol 2005;173(3):737–741. [PubMed: 15711259]
5. Sved PD, Gomez P, Manoharan M, Kim SS, Soloway MS. Limitations of biopsy Gleason grade: implications for counseling patients with biopsy Gleason score 6 prostate cancer. J Urol 2004;172(1): 98–102. [PubMed: 15201746]
6. Ung JO, San FranciscoIF, Regan MM, DeWolf WC, Olumi AF. The relationship of prostate gland volume to extended needle biopsy on prostate cancer detection. J Urol 2003;169(1):130–135. [PubMed: 12478120]
7. San Francisco IF, Regan MM, Olumi AF, DeWolf WC. Percent of cores positive for cancer is a better preoperative predictor of cancer recurrence after radical prostatectomy than prostate specific antigen. J Urol 2004;171(4):1492–1499. [PubMed: 15017206]
8. Krongrad A, Lai H, Lai S. Variation in prostate cancer survival explained by significant prognostic factors. J Urol 1997;158(4):1487–1490. [PubMed: 9302148]
9. Moul JW. Hormonal therapy options for biochemical recurrence of prostate cancer after local therapy. Mol Urol 2000;4(3):267–271. [PubMed: 11062383]discussion 73
10. D'Amico AV, Whittington R, Malkowicz SB, Wu YH, Chen M, Art M, Tomaszewski JE, Wein A. Combination of the preoperative PSA level, biopsy gleason score, percentage of positive biopsies, and MRI T-stage to predict early PSA failure in men with clinically localized prostate cancer. Urology 2000;55(4):572–577. [PubMed: 10736506]
11. Blackwell KL, Bostwick DG, Myers RP, Zincke H, Oesterling JE. Combining prostate specific antigen with cancer and gland volume to predict more reliably pathological stage: the influence of prostate specific antigen cancer density. J Urol 1994;151(6):1565–1570. [PubMed: 7514689]
12. Akimoto S, Masai M, Akakura K, Shimazaki J. Tumor marker doubling time in patients with prostate cancer: determination of prostate-specific antigen and prostatic acid phosphatase doubling time. Eur Urol 1995;27(3):207–212. [PubMed: 7541360]
13. Tsuji M, Murakami Y, Kanayama H, Sano T, Kagawa S. Immunohistochemical analysis of Ki-67 antigen and Bcl-2 protein expression in prostate cancer: effect of neoadjuvant hormonal therapy. Br J Urol 1998;81(1):116–121. [PubMed: 9467487]
14. Keshgegian AA, Johnston E, Cnaan A. Bcl-2 oncoprotein positivity and high MIB-1 (Ki-67) proliferative rate are independent predictive markers for recurrence in prostate carcinoma. Am J Clin Pathol 1998;110(4):443–449. [PubMed: 9763029]
15. Bonkhoff H, Fixemer T, Remberger K. Relation between Bcl-2, cell proliferation, and the androgen receptor status in prostate tissue and precursors of prostate cancer. Prostate 1998;34(4):251–258. [PubMed: 9496899]
16. Ahlgren G, Pedersen K, Lundberg S, Aus G, Hugosson J, Abrahamsson PA. Tumor cell proliferation in prostate cancer after 3 months of neoadjuvant LHRH analogue treatment is a prognostic marker of recurrence after radical prostatectomy. Urology 1999;54(2):329–334. [PubMed: 10443734]
17. Moul JW, Bettencourt MC, Sesterhenn IA, Mostofi FK, McLeod DG, Srivastava S, Bauer JJ. Protein expression of p53, bcl-2, and KI-67 (MIB-1) as prognostic biomarkers in patients with surgically treated, clinically localized prostate cancer. Surgery 1996;120(2):159–166. [PubMed: 8751578] discussion 66–7
18. Bock JL, Klee GG. How sensitive is a prostate-specific antigen measurement? How sensitive does it need to be? Arch Pathol Lab Med 2004;128(3):341–343. [PubMed: 14987148]
19. Beerlage HP. Alternative therapies for localized prostate cancer. Curr Urol Rep 2003;4(3):216–220. [PubMed: 12756085]

20. Zlotta AR, Djavan B MatosC, Noel JC, Peny MO, Silverman DE, Marberger M, Schulman CC. Percutaneous transperineal radiofrequency ablation of prostate tumour: safety, feasibility and pathological effects on human prostate cancer. Br J Urol 1998;81(2):265–275. [PubMed: 9488071]
21. Long JP. Cryosurgical ablation of the prostate: current technique and clinical outcomes. Surg Technol Int 2003;11:213–219. [PubMed: 12931304]
22. Papandreou CN, Logothetis CJ. Bortezomib as a potential treatment for prostate cancer. Cancer Res 2004;64(15):5036–5043. [PubMed: 15289299]
23. Prepelica KL, Okeke Z, Murphy A, Katz AE. Cryosurgical ablation of the prostate: high risk patient outcomes. Cancer 2005;103(8):1625–1630. [PubMed: 15747374]
24. Asatiani E, Gelmann EP. Targeted therapies for prostate cancer. Expert Opin Ther Targets 2005;9 (2):283–298. [PubMed: 15934916]
25. Kurhanewicz J, Swanson MG, Wood PJ, Vigneron DB. Magnetic resonance imaging and spectroscopic imaging: Improved patient selection and potential for metabolic intermediate endpoints in prostate cancer chemoprevention trials. Urology 2001;57(4 Suppl 1):124–128. [PubMed: 11295609]
26. Crawford ED, Fair WR, Kelloff GJ, Lieber MM, Miller GJ, Scardino PT, DeAntoni EP. Chemoprevention of prostate cancer: guidelines for possible intervention strategies. J Cell Biochem Suppl 1992;16H:140–145. [PubMed: 1337764]
27. Wang L, Mullerad M, Chen HN, Eberhardt SC, Kattan MW, Scardino PT, Hricak H. Prostate cancer: incremental value of endorectal MR imaging findings for prediction of extracapsular extension. Radiology 2004;232(1):133–139. [PubMed: 15166321]
28. Mettlin C, Lee F, Drago J, Murphy GP. The American Cancer Society National Prostate Cancer Detection Project. Findings on the detection of early prostate cancer in 2425 men. Cancer 1991;67 (12):2949–2958. [PubMed: 1710531]
29. Halpern EJ, Frauscher F, Strup SE, Nazarian LN, O'Kane P, Gomella LG. Prostate: high-frequency Doppler US imaging for cancer detection. Radiology 2002;225(1):71–77. [PubMed: 12354987]
30. Arger PH, Malkowicz SB, VanArsdalen KN, Sehgal CM, Holzer A, Schultz SM. Color and power Doppler sonography in the diagnosis of prostate cancer: comparison between vascular density and total vascularity. J Ultrasound Med 2004;23(5):623–630. [PubMed: 15154528]
31. Ito H, Kamoi K, Yokoyama K, Yamada K, Nishimura T. Visualization of prostate cancer using dynamic contrast-enhanced MRI: comparison with transrectal power Doppler ultrasound. Br J Radiol 2003;76(909):617–624. [PubMed: 14500276]
32. Yu KK, Hricak H. Imaging prostate cancer. Radiologic Clinics of North America 2000;38(1):59–85. [PubMed: 10664667]viii
33. Siegelman ES. Magnetic resonance imaging of the prostate. Seminars in Roentgenology 1999;34(4): 295–312. [PubMed: 10553605]
34. Cheng D, Tempany CM. MR imaging of the prostate and bladder. Seminars in Ultrasound, CT & MR 1998;19(1):67–89.
35. Seltzer SE, Getty DJ, Tempany CM, Pickett RM, Schnall MD, McNeil BJ, Swets JA. Staging prostate cancer with MR imaging: a combined radiologist-computer system. Radiology 1997;202(1):219–226. [PubMed: 8988214]
36. Epstein JI, Carmichael MJ, Pizov G, Walsh PC. Influence of capsular penetration on progression following radical prostatectomy: a study of 196 cases with long-term followup. J Urol 1993;150(1): 135–141. [PubMed: 7685422]
37. Bloch BN, Rofsky NM, Baroni RH, Marquis RP, Pedrosa I, Lenkinski RE. 3 Tesla magnetic resonance imaging of the prostate with combined pelvic phased-array and endorectal coils; Initial experience (1). Acad Radiol 2004;11(8):863–867. [PubMed: 15288036]
38. Cunningham CH, Vigneron DB, Marjanska M, Chen AP, Xu D, Hurd RE, Kurhanewicz J, Garwood M, Pauly JM. Sequence design for magnetic resonance spectroscopic imaging of prostate cancer at 3 T. Magn Reson Med 2005;53(5):1033–1039. [PubMed: 15844147]
39. Carroll PR, Coakley FV, Kurhanewicz J. Magnetic resonance imaging and spectroscopy of prostate cancer. Rev Urol 2006;8:S4–S10. [PubMed: 17021625]

40. Chen AP, Cunningham CH, Kurhanewicz J, Xu D, Hurd RE, Pauly JM, Carvajal L, Karpodinis K, Vigneron DB. High-resolution 3D MR spectroscopic imaging of the prostate at 3 T with the MLEV-PRESS sequence. Magn Reson Imaging 2006;24(7):825–832. [PubMed: 16916699]
41. Mueller-Lisse UG, Swanson MG, Vigneron DB, Kurhanewicz J. Magnetic resonance spectroscopy in patients with locally confined prostate cancer: association of prostatic citrate and metabolic atrophy with time on hormone deprivation therapy, PSA level, and biopsy Gleason score. Eur Radiol 2007;17 (2):371–378. [PubMed: 16791635]
42. Rajesh A, Coakley FV, Kurhanewicz J. 3D MR spectroscopic imaging in the evaluation of prostate cancer. Clin Radiol 2007;62(10):921–929. [PubMed: 17765456]
43. Westphalen AC, Coakley FV, Qayyum A, Swanson M, Simko JP, Lu Y, Zhao S, Carroll PR, Yeh BM, Kurhanewicz J. Peripheral Zone Prostate Cancer: Accuracy of Different Interpretative Approaches with MR and MR Spectroscopic Imaging. Radiology. 2007
44. Gonzalez RG, Schaefer PW, Buonanno FS, Schwamm LH, Budzik RF, Rordorf G, Wang B, Sorensen AG, Koroshetz WJ. Diffusion-weighted MR imaging: diagnostic accuracy in patients imaged within 6 hours of stroke symptom onset. Radiology 1999;210(1):155–162. [PubMed: 9885601]
45. Schaefer PW. Diffusion-weighted imaging as a problem-solving tool in the evaluation of patients with acute strokelike syndromes. Top Magn Reson Imaging 2000;11(5):300–309. [PubMed: 11142628]
46. Mardor Y, Roth Y, Lidar Z, Jonas T, Pfeffer R, Maier SE, Faibel M, Nass D, Hadani M, Orenstein A, Cohen JS, Ram Z. Monitoring response to convection-enhanced taxol delivery in brain tumor patients using diffusion-weighted magnetic resonance imaging. Cancer Res 2001;61(13):4971–4973. [PubMed: 11431326]
47. Song SK, Qu Z, Garabedian EM, Gordon JI, Milbrandt J, Ackerman JJ. Improved magnetic resonance imaging detection of prostate cancer in a transgenic mouse model. Cancer Res 2002;62(5):1555–1558. [PubMed: 11888935]
48. Jennings D, Hatton BN, Guo J, Galons JP, Trouard TP, Raghunand N, Marshall J, Gillies RJ. Early response of prostate carcinoma xenografts to docetaxel chemotherapy monitored with diffusion MRI. Neoplasia 2002;4(3):255–262. [PubMed: 11988845]
49. Maier SE, Gudbjartsson H, Patz S, Hsu L, Lovblad KO, Edelman RR, Warach S, Jolesz FA. Line scan diffusion imaging: characterization in healthy subjects and stroke patients. AJR Am J Roentgenol 1998;171(1):85–93. [PubMed: 9648769]
50. Robertson RL, Maier SE, Mulkern RV, Vajapayam S, Robson CD, Barnes PD. MR line-scan diffusion imaging of the spinal cord in children. AJNR Am J Neuroradiol 2000;21(7):1344–1348. [PubMed: 10954293]
51. Gudbjartsson H, Maier SE, Mulkern RV, Morocz IA, Patz S, Jolesz FA. Line scan diffusion imaging. Magn Reson Med 1996;36(4):509–519. [PubMed: 8892201]
52. Issa B. In vivo measurement of the apparent diffusion coefficient in normal and malignant prostatic tissues using echo-planar imaging. J Magn Reson Imaging 2002;16(2):196–200. [PubMed: 12203768]
53. Strohmeyer D, Rossing C, Strauss F, Bauerfeind A, Kaufmann O, Loening S. Tumor angiogenesis is associated with progression after radical prostatectomy in pT2/pT3 prostate cancer. Prostate 2000;42 (1):26–33. [PubMed: 10579796]
54. Borre M, Offersen BV, Nerstrom B, Overgaard J. Microvessel density predicts survival in prostate cancer patients subjected to watchful waiting. Br J Cancer 1998;78(7):940–944. [PubMed: 9764587]
55. Fregene TA, Khanuja PS, Noto AC, Gehani SK, Van Egmont EM, Luz DA, Pienta KJ. Tumor-associated angiogenesis in prostate cancer. Anticancer Res 1993;13(6B):2377–2381. [PubMed: 7510938]
56. Weidner N, Carroll PR, Flax J, Blumenfeld W, Folkman J. Tumor angiogenesis correlates with metastasis in invasive prostate carcinoma. Am J Pathol 1993;143(2):401–409. [PubMed: 7688183]
57. Brawer MK, Deering RE, Brown M, Preston SD, Bigler SA. Predictors of pathologic stage in prostatic carcinoma. The role of neovascularity. Cancer 1994;73(3):678–687. [PubMed: 7507798]
58. Silberman MA, Partin AW, Veltri RW, Epstein JI. Tumor angiogenesis correlates with progression after radical prostatectomy but not with pathologic stage in Gleason sum 5 to 7 adenocarcinoma of the prostate. Cancer 1997;79(4):772–779. [PubMed: 9024715]

59. Hall MC, Troncoso P, Pollack A, Zhau HY, Zagars GK, Chung LW, von Eschenbach AC. Significance of tumor angiogenesis in clinically localized prostate carcinoma treated with external beam radiotherapy. Urology 1994;44(6):869–875. [PubMed: 7527168]
60. Gettman MT, Pacelli A, Slezak J, Bergstralh EJ, Blute M, Zincke H, Bostwick DG. Role of microvessel density in predicting recurrence in pathologic Stage T3 prostatic adenocarcinoma. Urology 1999;54(3):479–485. [PubMed: 10475358]
61. Rubin MA, Buyyounouski M, Bagiella E, Sharir S, Neugut A, Benson M, de la Taille A, Katz AE, Olsson CA, Ennis RD. Microvessel density in prostate cancer: lack of correlation with tumor grade, pathologic stage, and clinical outcome. Urology 1999;53(3):542–547. [PubMed: 10096381]
62. Moul JW. Angiogenesis, p53, bcl-2 and Ki-67 in the progression of prostate cancer after radical prostatectomy. Eur Urol 1999;35(5–6):399–407. [PubMed: 10325496]
63. Schlemmer HP, Merkle J, Grobholz R, Jaeger T, Michel MS, Werner A, Rabe J, van Kaick G. Can pre-operative contrast-enhanced dynamic MR imaging for prostate cancer predict microvessel density in prostatectomy specimens? Eur Radiol 2004;14(2):309–317. [PubMed: 14531000]
64. Parker GJ, Suckling J, Tanner SF, Padhani AR, Revell PB, Husband JE, Leach MO. Probing tumor microvascularity by measurement, analysis and display of contrast agent uptake kinetics. J Magn Reson Imaging 1997;7(3):564–574. [PubMed: 9170043]
65. Parker GJ, Baustert I, Tanner SF, Leach MO. Improving image quality and T(1) measurements using saturation recovery turboFLASH with an approximate K-space normalisation filter. Magn Reson Imaging 2000;18(2):157–167. [PubMed: 10722976]
66. Tofts PS. Modeling tracer kinetics in dynamic Gd-DTPA MR imaging. J Magn Reson Imaging 1997;7 (1):91–101. [PubMed: 9039598]
67. Parker GJ, Tofts PS. Pharmacokinetic analysis of neoplasms using contrast-enhanced dynamic magnetic resonance imaging. Top Magn Reson Imaging 1999;10(2):130–142. [PubMed: 10551628]
68. Brasch RC, Li KC, Husband JE, Keogan MT, Neeman M, Padhani AR, Shames D, Turetschek K. In vivo monitoring of tumor angiogenesis with MR imaging. Acad Radiol 2000;7(10):812–823. [PubMed: 11048879]
69. Furman-Haran E, Grobgeld D, Kelcz F, Degani H. Critical role of spatial resolution in dynamic contrast-enhanced breast MRI. J Magn Reson Imaging 2001;13(6):862–867. [PubMed: 11382945]
70. Degani H, Gusis V, Weinstein D, Fields S, Strano S. Mapping pathophysiological features of breast tumors by MRI at high spatial resolution. Nat Med 1997;3(7):780–782. [PubMed: 9212107]
71. Huch, BoniRA.; Boner, JA.; Debatin, JF.; Trinkler, F.; Knonagel, H.; Von Hochstetter, A.; Helfenstein, U.; Krestin, GP. Optimization of prostate carcinoma staging: comparison of imaging and clinical methods. Clin Radiol 1995;50(9):593–600. [PubMed: 7554732]
72. Brown G, Macvicar DA, Ayton V, Husband JE. The role of intravenous contrast enhancement in magnetic resonance imaging of prostatic carcinoma. Clin Radiol 1995;50(9):601–606. [PubMed: 7554733]
73. Jager GJ, Ruijter ET, van de Kaa CA, de la Rosette JJ, Oosterhof GO, Thornbury JR, Ruijs SH, Barentsz JO. Dynamic TurboFLASH subtraction technique for contrast-enhanced MR imaging of the prostate: correlation with histopathologic results. Radiology 1997;203(3):645–652. [PubMed: 9169683]
74. Quinn SF, Franzini DA, Demlow TA, Rosencrantz DR, Kim J, Hanna RM, Szumowski J. MR imaging of prostate cancer with an endorectal surface coil technique: correlation with whole-mount specimens. Radiology 1994;190(2):323–327. [PubMed: 8284376]
75. Engelbrecht MR, Huisman HJ, Laheij RJ, Jager GJ, van Leenders GJ, Hulsbergen-Van De Kaa CA, de la Rosette JJ, Blickman JG, Barentsz JO. Discrimination of prostate cancer from normal peripheral zone and central gland tissue by using dynamic contrast-enhanced MR imaging. Radiology 2003;229 (1):248–254. [PubMed: 12944607]
76. Ogura K, Maekawa S, Okubo K, Aoki Y, Okada T, Oda K, Watanabe Y, Tsukayama C, Arai Y. Dynamic endorectal magnetic resonance imaging for local staging and detection of neurovascular bundle involvement of prostate cancer: correlation with histopathologic results. Urology 2001;57(4): 721–726. [PubMed: 11306390]
77. Bloch BN, Furman-Haran E, Helbich TH, Lenkinski RE, Degani H, Kratzik C, Susani M, Haitel A, Jaromi S, Ngo L, Rofsky NM. Accurate Determination of Extracapsular Extension in Prostate Cancer

using High Resolution Dynamic Contrast Enhanced and T2-W Magnetic Resonance Imaging: Initial Results. Radiology. 2007accepted for publication

78. Bloch BN, Lenkinski RE, Helbich TH, Ngo L, Oismueller R, Jaromi S, Kubin K, Hawliczek R, Kaplan ID, Rofsky NM. Prostate postbrachytherapy seed distribution: Comparison of high-resolution, contrast-enhanced, T1- and T2-weighted endorectal magnetic resonance imaging versus computed tomography: Initial experience. Int J Radiat Oncol Biol Phys. 2007
79. Rosen Y, Bloch BN, Lenkinski RE, Greenman RL, Marquis RP, Rofsky NM. 3T MR of the prostate: reducing susceptibility gradients by inflating the endorectal coil with a barium sulfate suspension. Magn Reson Med 2007;57(5):898–904. [PubMed: 17457870]
80. Veltri RW, Miller MC, Mangold LA, O'Dowd GJ, Epstein JI, Partin AW. Prediction of pathological stage in patients with clinical stage T1c prostate cancer: the new challenge. J Urol 2002;168(1):100–104. [PubMed: 12050500]
81. Han M, Partin AW. Nomograms for clinically localized prostate cancer. Part I: radical prostatectomy. Semin Urol Oncol 2002;20(2):123–130. [PubMed: 12012298]
82. Partin AW, Mangold LA, Lamm DM, Walsh PC, Epstein JI, Pearson JD. Contemporary update of prostate cancer staging nomograms (Partin Tables) for the new millennium. Urology 2001;58(6): 843–848. [PubMed: 11744442]
83. Chon CH, Lai FC, McNeal JE, Presti JC Jr. Use of extended systematic sampling in patients with a prior negative prostate needle biopsy. J Urol 2002;167(6):2457–2460. [PubMed: 11992057]
84. Lopez-Corona E, Ohori M, Scardino PT, Reuter VE, Gonen M, Kattan MW. A nomogram for predicting a positive repeat prostate biopsy in patients with a previous negative biopsy session. J Urol 2003;170(4 Pt 1):1184–1188. [PubMed: 14501721]discussion 8
85. Hong YM, Lai FC, Chon CH, McNeal JE, Presti JC Jr. Impact of prior biopsy scheme on pathologic features of cancers detected on repeat biopsies. Urol Oncol 2004;22(1):7–10. [PubMed: 14969796]
86. Lenkinski RE, Bloch BN, Liu F, Frangioni JV, Perner S, Rubin MA, Genega EM, Rofsky NM, Gaston SM. Correlation of MRI/MRS Parameters with Genetic Over-expression Profiles In Human Prostate Cancer. MAGMA. 2008(submitted)

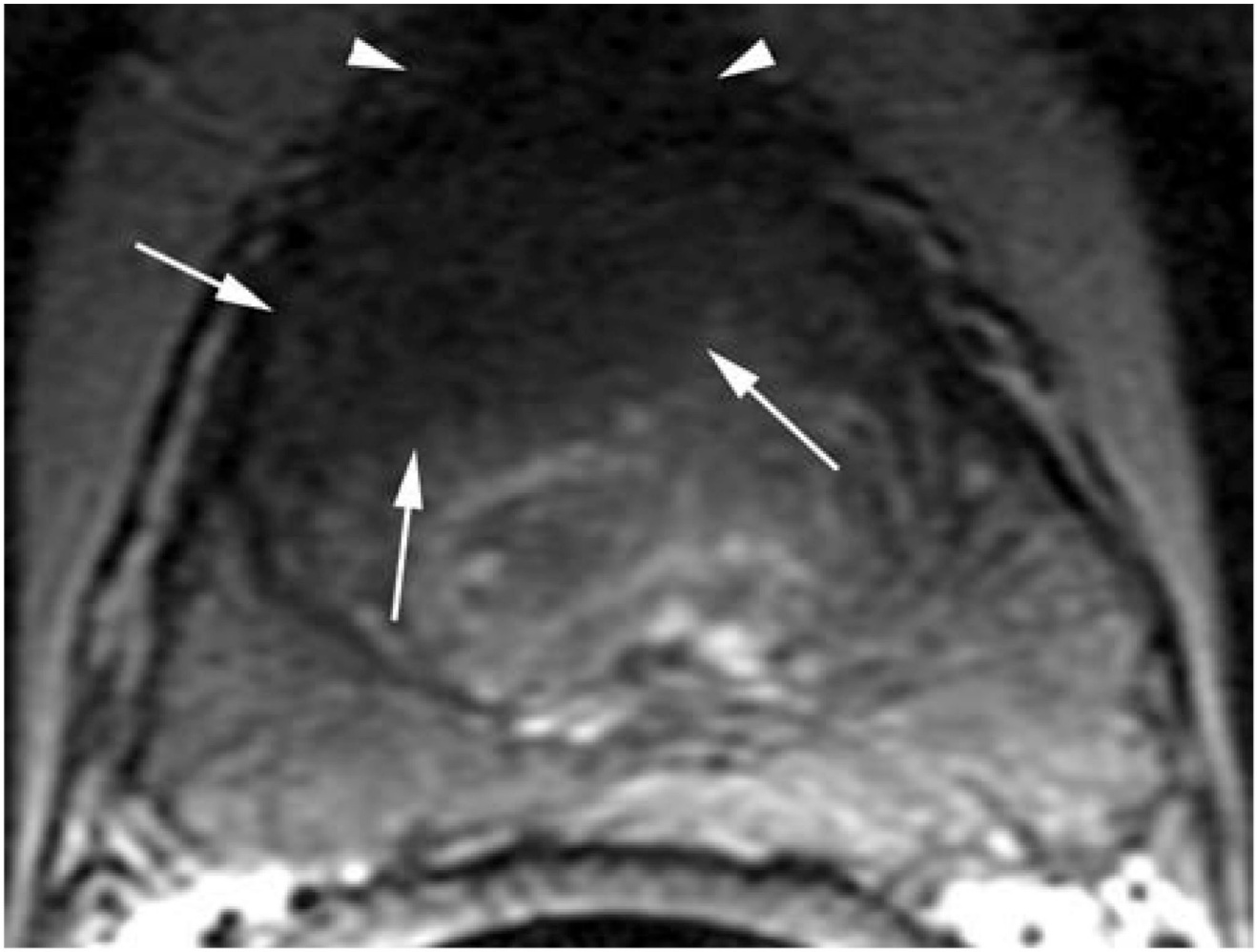

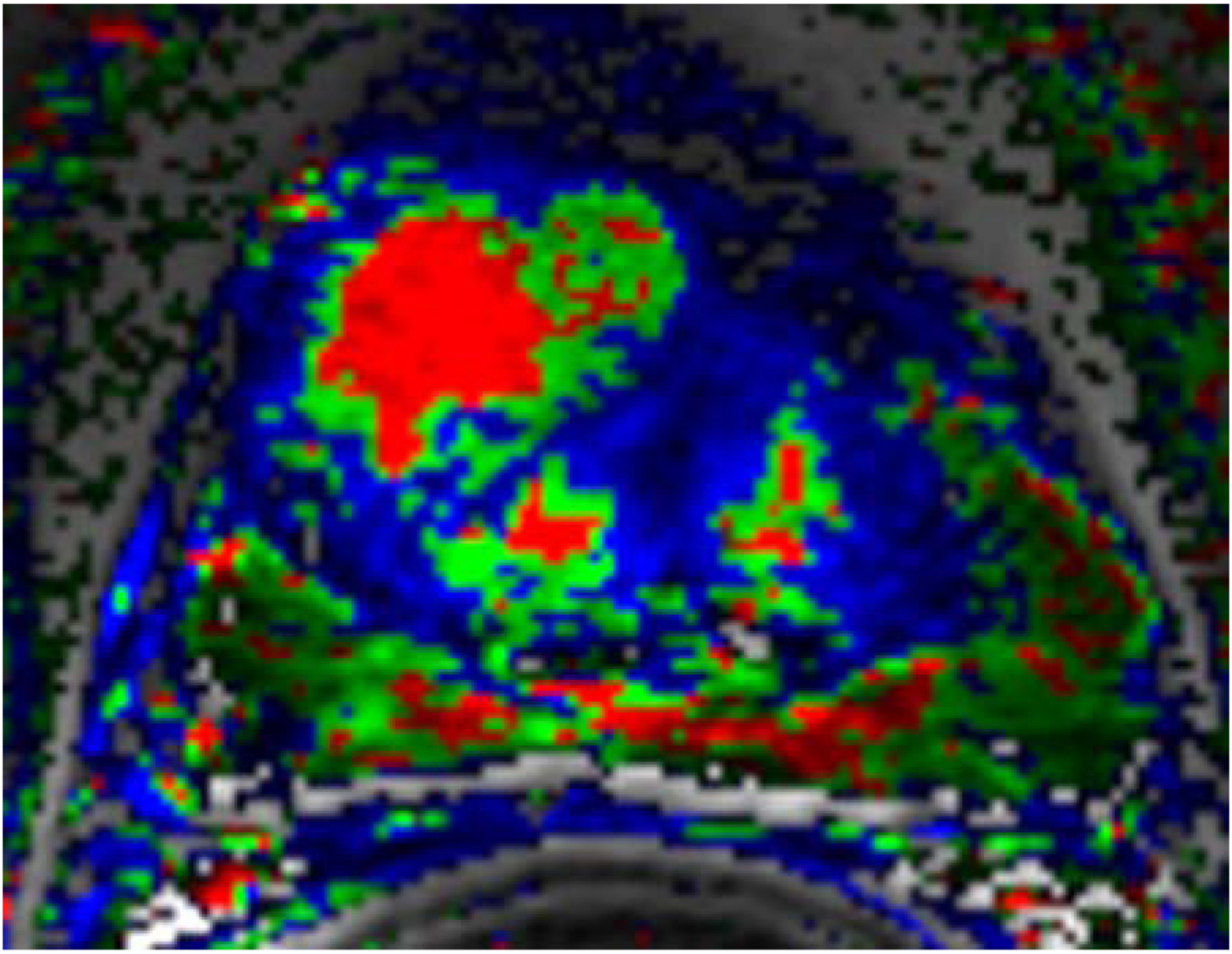

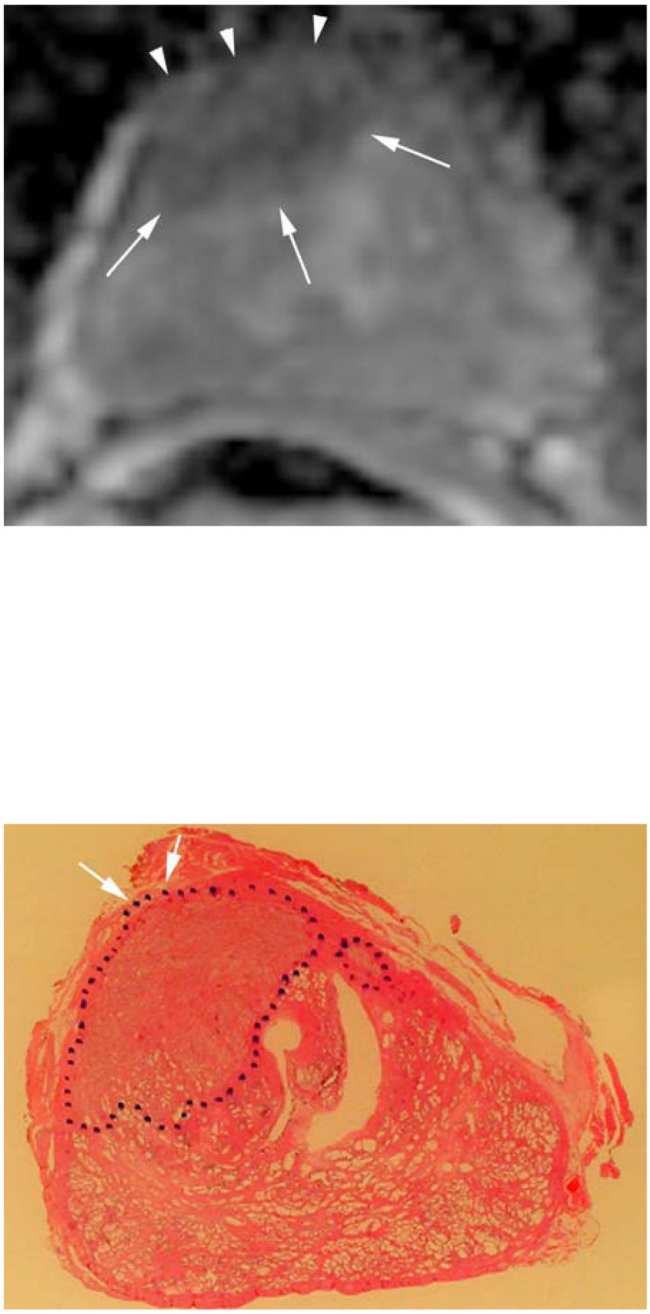

Figure 1.
T2-W MRI and DCE-MRI based, color-coded image in correlation with whole mount histopathology of a 56 year old patient with repeat negative biopsies and rising PSA. A third saturation biopsy prompted by the MRI was positive in 3/20 cores.
a. Axial T2-W FSE (5800/1600) 2.2-mm-thick image of the mid-third of the prostate. Note the large hypointense area in the anterior portion of the gland (white arrows). The tumor abuts the fibromuscular band and is ill-defined at the right anterior aspect. With poor delineation between the aspect. With poor delineation between the fibromuscular band/pseudo-capsule, the tumor was staged as T3a (white arrowheads).

b. Corresponding color-coded DCE 3D-Gradient-Echo (6.9/2.1) 2.6-mm-thick image showed cancer (geographic area with confluent bright red pixilation) predominantly in the anterior gland. In this case the DCE MRI underestimates the tumor extend. However, the combined analysis of T2-W and DCE MRI yielded a MRI stage of T3a.
c. Corresponding apparent diffusion coefficient (ADC) map of DWI, which shows a parametric image containing the apparent diffusion coefficients of diffusion weighted images. Note the area with reduced ADC values suggesting tumor in the anterior gland (white arrows) with ECE (white arrow heads).
d. Whole mount histopathology proved cancer (black dotted lines) predominately on the right side. And stage T3a with ECE right anteriorly (white short arrows).

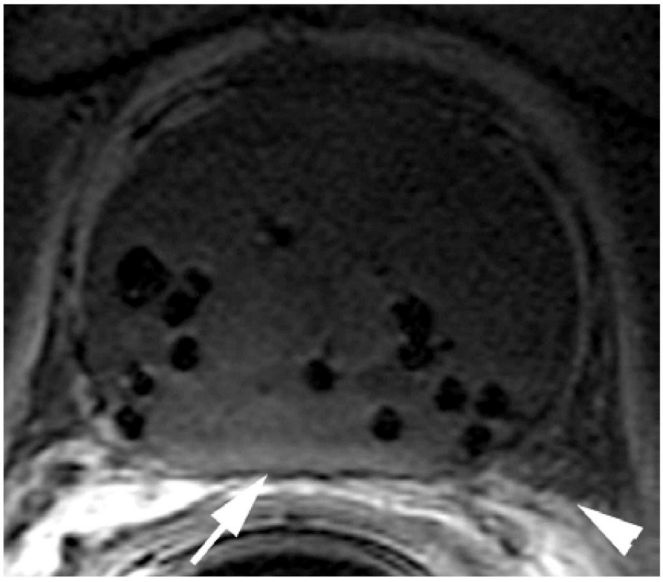

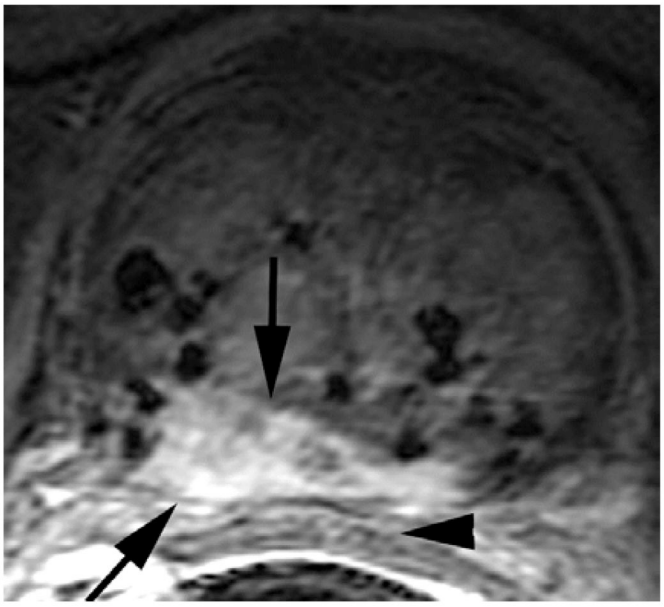

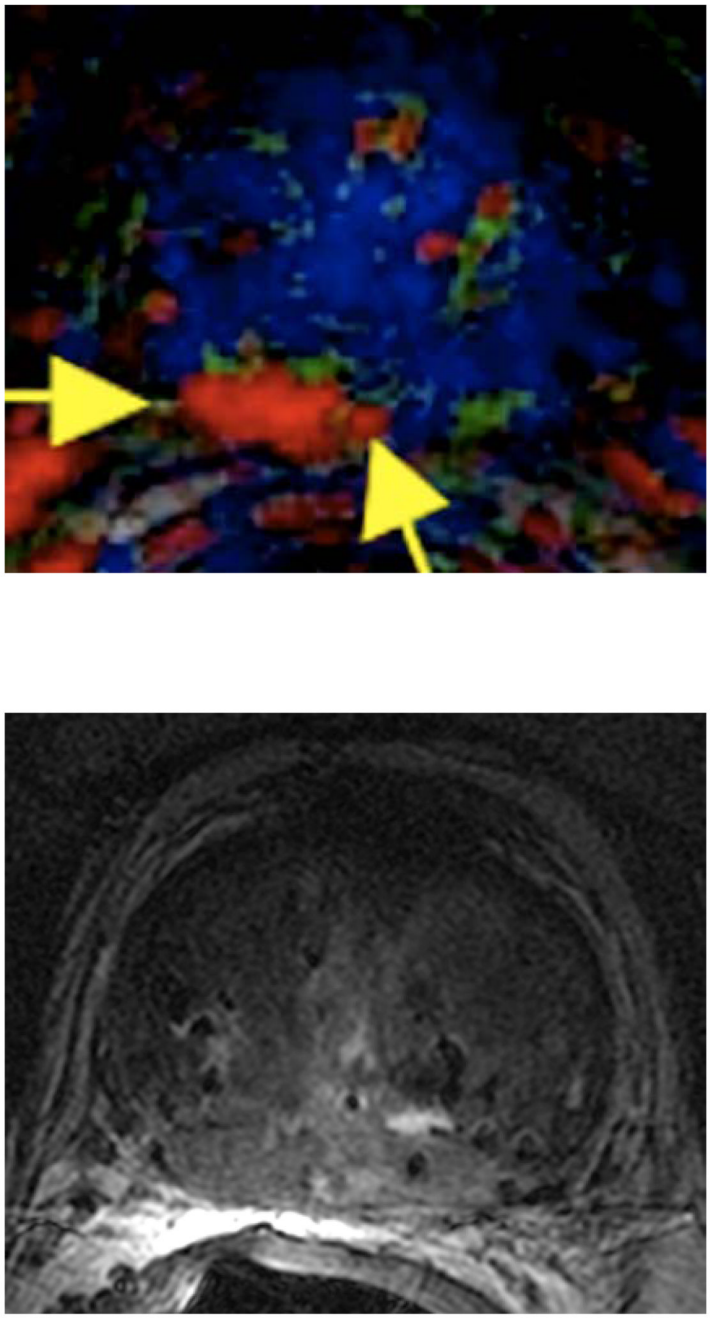

Figure 2.

a. DCE 3D-Gradient-Echo (6.9/2.1) 2.6-mm-thick pre-contrast image: Note the signal voids (seeds) and the clear depiction of prostate capsule (white arrow) and neurovascular bundles (arrow head).

b. Corresponding DCE 3D-Gradient-Echo (6.9/2.1) 2.6-mm-thick early post-contrast image. Note the tumor showing early wash-in (black arrows) on the background of relatively low perfusion of the radiated gland. The Brachytherapy seeds are represented as focal signal voids. Note also the proximity of the tumor to the rectal wall (black arrowhead).

c. Corresponding color-coded DCE 3D-Gradient-Echo (6.9/2.1) 2.6-mm-thick image showed cancer (geographic area with confluent bright red pixilation) in the right posterior peripheral zone (yellow arrows).
d. Axial T2-W FSE (5800/160) 2.2-mm-thick image of the mid-third of the prostate. (Corresponding to Fig. 1 a, b). Note that the entire prostate gland shows low signal due to post radiation changes, and therefore, the tumor cannot be delineated.

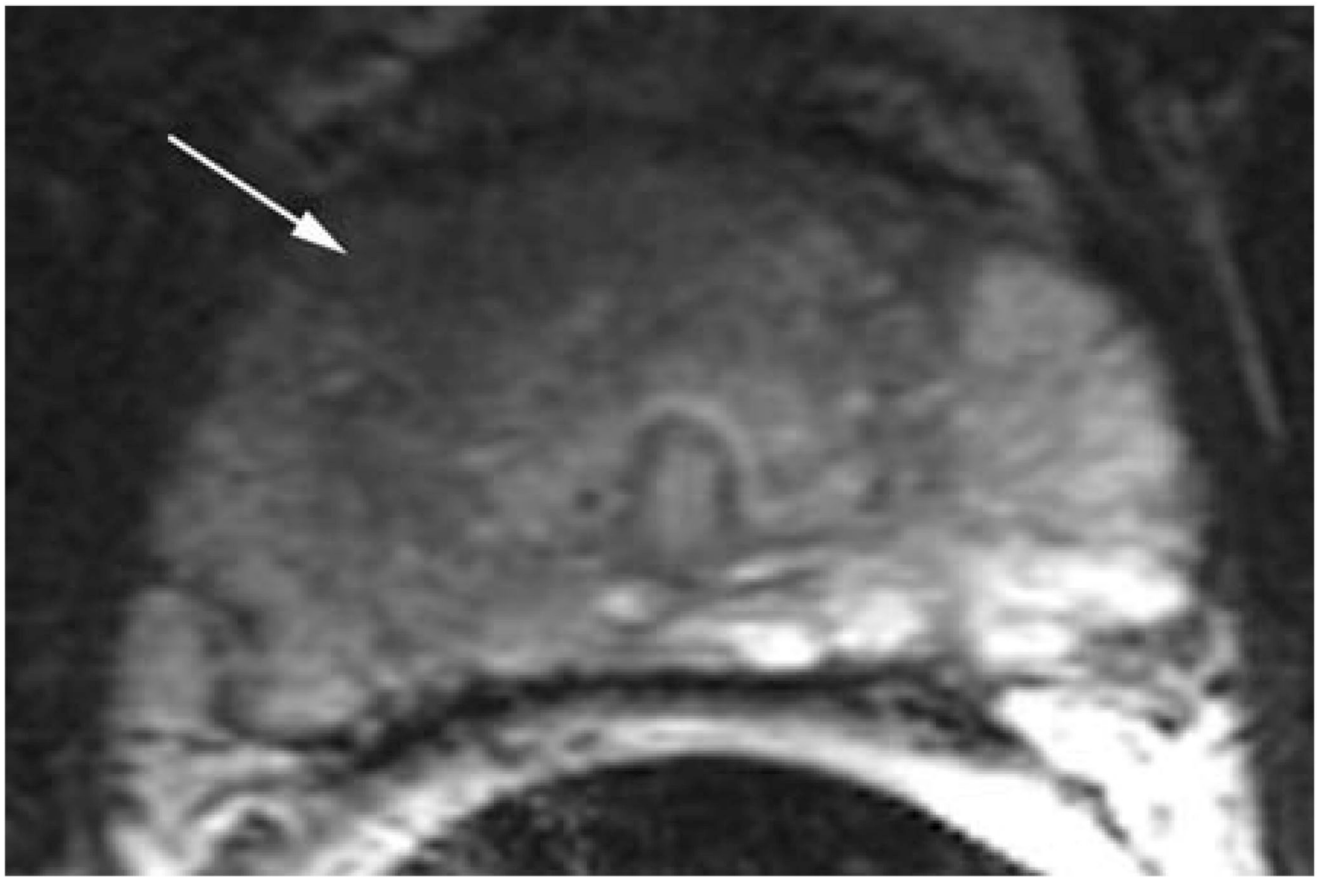

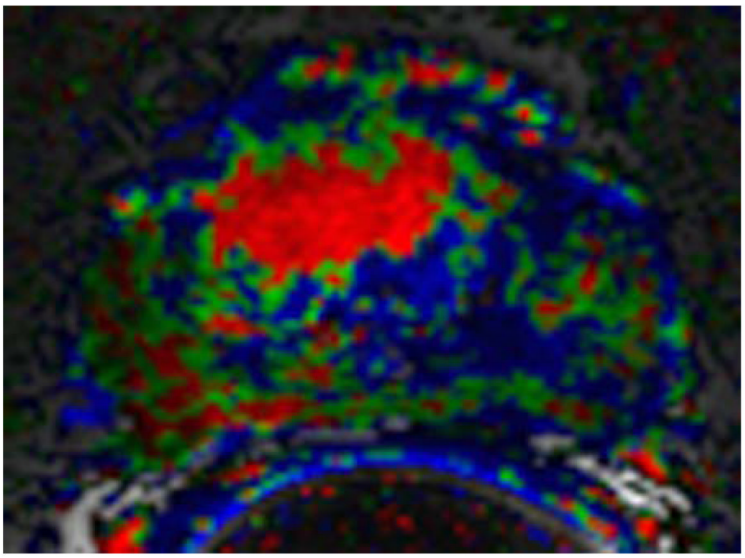

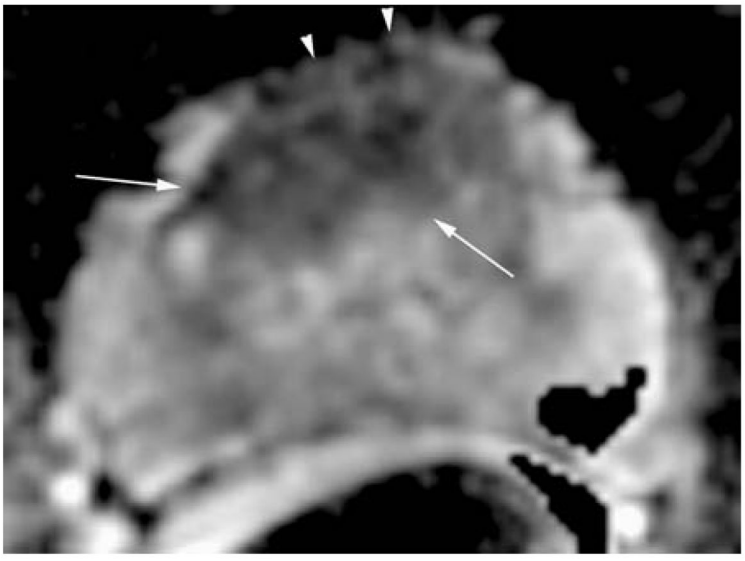

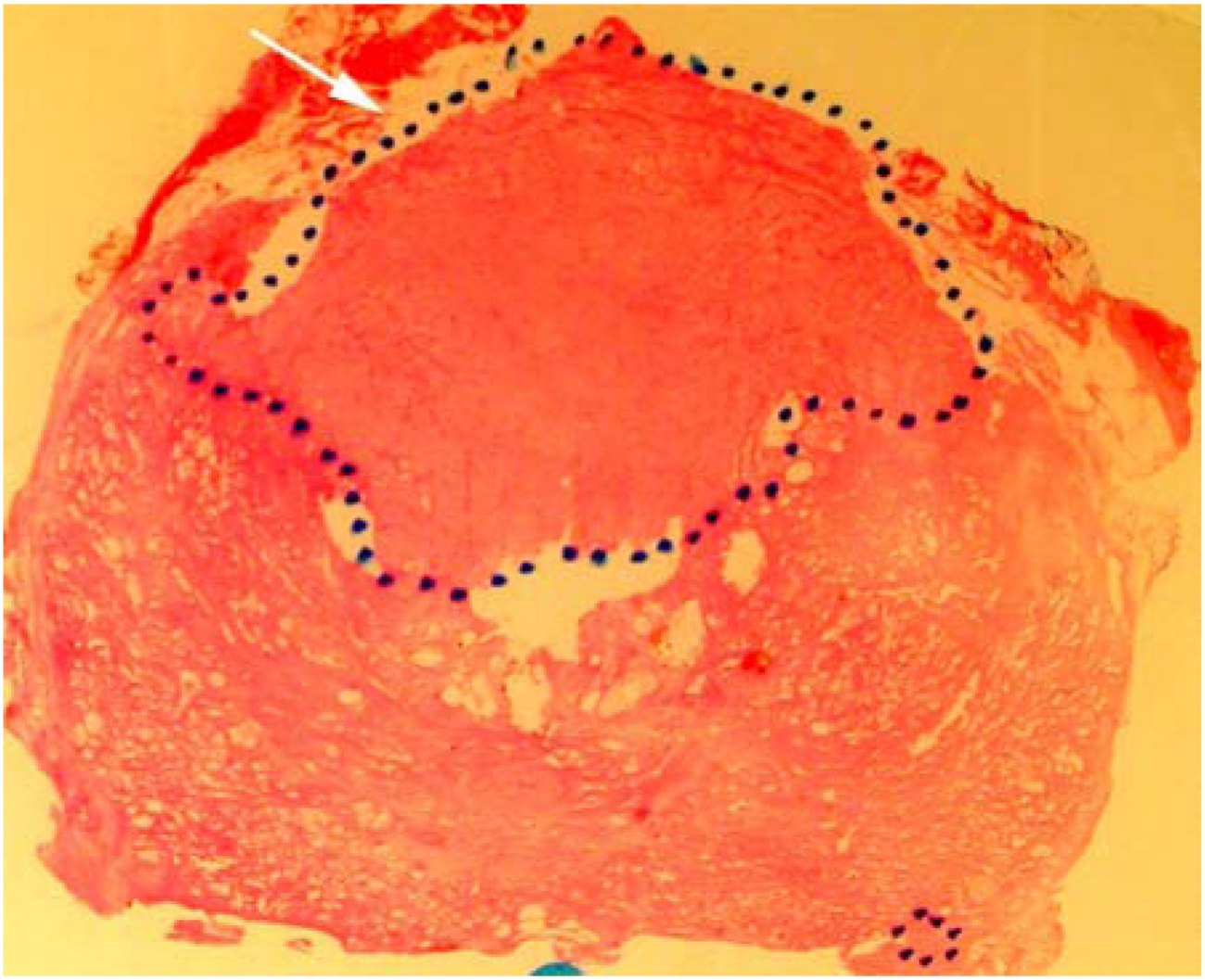

Figure 3.

a. Axial T2-W FSE (7050/156) 2.2-mm-thick image of the mid-third of the prostate. Note the subtle hypointense area in the anterior aspect of the gland (white arrow) - the cancer is not readily seen.

b. Corresponding color-coded DCE 3D-Gradient-Echo (6.9/2.1) 2.6-mm-thick image. Note the large anterior tumor easily seen in bright red, adjacent to the pseudo-capsule.

c. Corresponding apparent diffusion coefficient (ADC) map of a 3.0mm thick DWI. Note the area with reduced ADC values suggesting tumor in the anterior gland (white arrows), involvement of the fibromuscular band and suspected ECE (white arrow heads).

d. Whole mount histopathology proved cancer (black dotted line) in the anterior gland, with a final pathologic stage pT3a with minimal ECE right anteriorly (white arrow) – as reported by MRI.

Table 1

BIDMC Imaging parameters at 3 Tesla

Sequence:	T1-W (SE or FSE)	T2-W FSE	T2-W FSE	High spatial resolution 3D GE	(DWI-EPI)
Imaging Plane:	Axial	Axial	Coronal	Axial	Axial
Coil(s):	Combined Torso Phased Array and Endo Rectal	Combined Torso Phased Array and Endo Rectal	Combined Torso Phased Array and Endo Rectal	Combined Torso Phased Array and Endo Rectal	Combined Torso Phased Array and Endo Rectal
Anatomic Coverage:	Aortic Bifurcation to Symphysis Pubis	Prostate and seminal vesicles	Prostate and seminal vesicles	Prostate and seminal vesicles	Prostate and seminal vesicles
TE (msec):	12	165	165	2.1	80.6
TR (msec):	600–700	6375	7600	7.1	6500
Slice Thickness /Spacing (Gap) (mm):	5/1	1.5–2/0	2/0	2–3/0; larger sections used for larger glands*	3/0
Field Of View (FOV) (cm):	28–22	12	14	12	24
Frequency Direction:	Transverse	AP	AP or SI	AP	AP
Matrix:	256×192	320 × 224–192	320× 224–192	256×224	256 ×192
NEX:	1	5	5	2	2
Echo Train Length (ETL):		22	22		
Acquisition time	5 min	5–7min	5–6 min	1 min 32 sec each × 7 = 10 min 44 sec total	7 min
Flip Angle:				18°	
Receiver Bandwidth:		31.25 kHz	31.25 kHz	20.83 kHz	
Notes:	Frequency: Transverse to prevent endorectal coil motion artifact from obscuring pelvic nodes.	Frequency: AP to prevent endorectal coil motion artifact from obscuring the prostate gland.		Frequency: AP to prevent endorectal coil motion artifact from obscuring the prostate gland	Number of Directions= 25** B-value:0; 1000

* Constraint – maintain each DCE MRI 3D data set with temporal resolution at ~ 90–95 sec for the parametric/kinetic analysis.

** Instead of choosing more NEX (averages) we use more directions, to achieve not only better SNR but also improved results in diffusion tensor imaging and anisotropic maps as well as enhanced contrast in the ADC maps.